Effect on Landau damping rates for a non-Maxwellian distribution function consisting of two electron populations*

M. N. S. Qureshi[a)b)†], S. Sehar[b)], H. A. Shah[b)], and J. B. Cao[a)]

[a)] *Space Science Institute, Beihang University, Beijing* 100191, *China*
[b)] *Department of Physics, Government College University, Lahore* 54000, *Pakistan*

(Received 4 May 2012; revised manuscript received 1 November 2012)

In many physical situations where a laser or electron beam passes through a dense plasma, hot low-density electron populations can be generated, resulting in a particle distribution function consisting of a dense cold population and a small hot population. Presence of such low-density electron distributions can alter the wave damping rate. A kinetic model is employed to study the Landau damping of Langmuir waves when a small hot electron population is present in the dense cold electron population with non-Maxwellian distribution functions. Departure of plasma from Maxwellian distributions significantly alters the damping rates as compared to the Maxwellian plasma. Strong damping is found for highly non-Maxwellian distributions as well as plasmas with a higher density and hot electron population. Existence of weak damping is also established when the distribution contains broadened flat tops at the low energies or tends to be Maxwellian. These results may be applied in both experimental and space physics regimes.

Keywords: Landau damping, Langmuir waves, two electron populations, non-Maxwellian distribution function

PACS: 52.27.Cm, 52.35.Fp, 94.20.Wj **DOI:** 10.1088/1674-1056/22/3/035201

1. Introduction

Landau, in his elegant paper[1], showed that resonant interaction of a wave with particles resulted in the collisionless damping of the electrostatic waves. Such Landau damping increases significantly when the distribution functions contain superthermal particles and shoulders in the distribution function profile.[2,3] Electron velocity distribution functions (VDFs) with pronounced superthermal tails[4–7] and flat tops (shoulders in the profile of distribution function)[8–11] are frequently observed in space plasmas, which are often modelled by κ or generalized (r, q) distribution functions.[12–15] Initially, the use of κ-like distribution was criticized due to the lack of its formal derivation. A classical analysis addressing this problem was presented by Hasegawa *et al*.[16] who demonstrated how the kappa distributions emerge as a natural consequence of the presence of superthermal radiation fields in plasmas. A kinetic theory has been developed, showing that κ-like velocity space distributions present a particular thermodynamic equilibrium state called the 'nonextensive' entropy, in which κ-like distributions are natural thermodynamic equilibrium solutions.[17,18] Collier[19] considers the generation of κ-like distributions using the velocity space Levy flights.

In plasmas, a small population of electrons possessing much higher energies than the original laser beam can be produced in the laboratory.[20,21] Simulation results of electron or laser beam propagation in dense plasmas often show electron distributions that are characterized by power-law tails of hot electrons superposed on an approximately Maxwellian bulk distribution.[22,23] The presence of such low density electron distributions can increase the wave damping rate. However, significant reduction in the electron plasma wave Landau damping rates has also been found while studying the behaviour of plasma waves using the kinetic theory in nonuniform heated large scale plasmas.[24] Yoon *et al*.[25] considered the self-consistent generation of superthermal electrons by beam–plasma interaction within the context of plasma kinetic theory.

Observations of electron VDFs from solar wind showed significant deviations from the Maxwellian distribution function, i.e., a dense thermal core and a hot superthermal population 'halo' can be distinguished in a slow solar wind.[26–30] It is now believed that the core corresponds to the relatively cool population, which is trapped within the potential of heliosphere, whereas the halo is composed of electrons energetic enough to escape this potential barrier.[31,32] Such electron VDFs cannot be modelled by distributions containing simply one electron population. In this context, Nieves-Chinchilla and Vinas[33] fitted a large number of samples of electron VDFs observed in the solar wind by a model distribution function composed of a bulk Maxwellian superimposed by a kappa distribution function.

In addition to the presence of κ-like electron VDFs, distributions have also been observed in space plasmas with flat tops. First observations of flat top (shoulders in the profile of

*Project supported by the National Natural Science Foundation of China (Grant No. 40931054), the National Basic Research Program of China (Grant No. 2011CB811404), and the Higher Education Commission of China (Grant No. 20-1886/R&D/10).

†Corresponding author. E-mail: nouman_sarwar@yahoo.com

distribution function) electron VDFs from the Vela 4 magnetosheath crossing were reported by Montgomery.[10] Flat top electron VDFs were also reported by Montgomery[11] using Vela 4 data during the crossing of the Earth's bow shock from the solar wind to the magnetosheath. During the ISEE 2 crossing of the Earth's bow shock, Feldman *et al.*[8] observed flat top electron VDFs. Feldman *et al.*[9] also reported the ISEE 3 observations of flat top electron VDFs from the weak and strong interplanetary shocks. Parks *et al.*[34] observed the flat top electron velocity distribution functions in the magnetotail with CLUSTER observations. By numerically solving the weak turbulence kinetic equations, Gaelzer *et al.*[30] showed that the self-consistent electron VDFs have characteristic flat top distributions with tenuous high-energy tails superimposed on Maxwellian distribution.

In recent years, electrostatic waves have been studied not only with fluid models,[35–39] but also with kinetic models[40–43] in different plasma regimes. However, most of the studies were based on Maxwellian plasmas. To the best of our knowledge, it is for the first time that in this paper, we study the Landau damping of Langmuir waves with a generalized (r, q) distribution function consisting of two electron populations, a hot superthermal population, and a cold bulk population. Limiting cases of generalized (r, q) distribution function have also been presented in the form of kappa and Maxwellian distributions. By employing such a two-component non-Maxwellian distribution, we study the effects on Landau damping rates when a dense thermal core is superimposed by high-energy tails in view of space and laboratory plasmas. Apart from the above-mentioned theoretical considerations, it may be noted that there are many instances of observations of Langmuir waves. These waves have been observed by FREJA and SCIFER satellites in the auroral zone,[44] and also by the satellite wind in the upstream region of the Earth's bow shock and interplanetary shocks,[45,46] while ULYSSES has given similar observations for the solar wind.[47,48]

2. Generalized (r, q) distribution function

The generalized (r, q) distribution function as a sum of a fractional hot and a cold bulk electron distribution takes the form

$$f_{rq}(v) = \frac{(1-F)C}{\pi}\left(\frac{a}{DT_c}\right)^{3/2}\left[1+\frac{1}{q-1}\left(\frac{a}{D^2}\frac{v^2}{T_c}\right)^{r+1}\right]^{-q} + \frac{FC}{\pi}\left(\frac{a}{DT_h}\right)^{3/2}\left[1+\frac{1}{q-1}\left(\frac{a}{D^2}\frac{v^2}{T_h}\right)^{r+1}\right]^{-q}, \quad (1)$$

where

$$C = \frac{3(q-1)^{-3/2(1+r)}\Gamma(q)}{4\Gamma\left(q-\frac{3}{2(1+r)}\right)\Gamma\left(1+\frac{3}{2(1+r)}\right)}, \quad (2)$$

and

$$D = \frac{3(q-1)^{-1/(1+r)}\Gamma\left(q-\frac{3}{2(1+r)}\right)\Gamma\left(\frac{3}{2(1+r)}\right)}{\Gamma\left(q-\frac{5}{2(1+r)}\right)\Gamma\left(\frac{5}{2(1+r)}\right)}. \quad (3)$$

where Γ is the usual Gamma function, T_c and T_h are the cold and hot electron temperature, respectively, and $a = m/2k_B$ with m being the electron mass and k_B the Boltzmann constant. The total electron density is the sum of the hot ($n_h = NF$) and cold ($n_c = N(1-F)$) electron densities, respectively. In the limit $r = 0$ and $q = \kappa + 1$, equation (1) is reduced to κ-distribution function, while in the limiting case of $r = 0$ and $q \to \infty$, it is reduced to the classical Maxwellian distribution function. The spectral indices r and q are bounded by the conditions: $q > 1$ and $q(1+r) > 5/2$, which arise from the normalization and definition of temperature for the distribution function. In general, r is the measure of the flat part or shoulders of the distribution at low energies, and q is the strength of the high energy tail, respectively.

Figures 1 and 2 show the profiles of generalized (r, q) distribution function for a 1% hot population at 10 eV added to cold dense population at 1 eV for different values of spectral indices r and q, respectively. Figure 1 is plotted for different values of spectral index q when r =1. From Fig. 1, we note that as the value of q increases, the high-energy tail decreases, distribution tends to become Maxwellian, and effect of two temperatures becomes more prominent, as exhibited through the second shoulder in the profile of distribution function. Figure 2 is plotted for different values of spectral index r when $q = 2$. For $q = 2$, we note that as r increases, not only the shoulders in the profile of distribution function becomes more broad, but the effect of two populations is enhanced and the high-energy tail decreases. Therefore, from Figs. 1 and 2, we can note that when q increases, the high-energy tail decreases, and when r increases, shoulders or the flat top in the profile of distribution become more prominent along with the enhancement in the two populations in both cases.

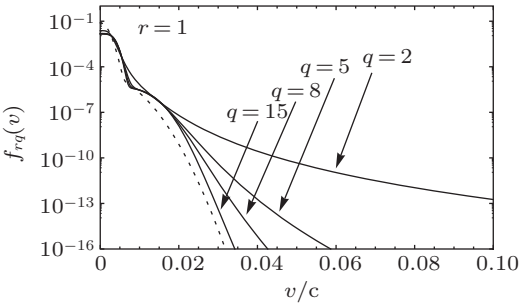

Fig. 1. Profile of generalized (r, q) distribution function for different values of q when $r = 1$ for $F = 0.01$, $T_c = 1$ eV, and $T_h = 10$ eV.

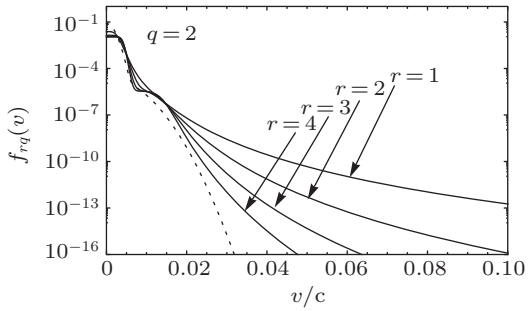

Fig. 2. Profile of generalized (r, q) distribution for different values of r when $q = 2$. The other parameters are the same as that of Fig. 1.

3. Dispersion relation

We follow the general formulism of kinetic theory to derive the dispersion relation for the electrostatic waves with complex frequency $\omega = \omega_r + i\omega_i$ and real wave number k. We consider the case of high-frequency electrostatic waves, where ion dynamics is not important. This procedure yields the propagation and damping characteristics of electron plasma (Langmuir) waves. Langmuir waves occur in a variety of plasmas including the laboratory plasmas, auroral zone, Earth's electron foreshock, and solar wind. In this paper, we investigate the dispersion relation and damping rates for the Langmuir waves in a plasma which is modelled by two-temperature generalized (r, q) distribution function in the limiting case of $k\lambda_D \ll 1$, where

$$\lambda_D = \left(\frac{T_c}{4\pi N e^2}\right)^{1/2} = \left(\frac{(q-1)^{1/(1+r)}\Gamma\left(q-\frac{5}{2(1+r)}\right)\Gamma\left(\frac{5}{2(1+r)}\right)}{3\Gamma\left(q-\frac{3}{2(1+r)}\right)\Gamma\left(\frac{3}{2(1+r)}\right)}\right)^{1/2} \times \left(\frac{\psi_{thc}}{\omega_p}\right) \quad (4)$$

is the electron Debye length,

$$\psi_{thc} = \left\{(T_c/m)\left(\frac{3(q-1)^{-1/(1+r)}\Gamma[q-3/2(1+r)]\Gamma[3/2(1+r)]}{\Gamma[q-5/2(1+r)]\Gamma[5/2(1+r)]}\right)\right\}^{1/2}$$

is the generalized electron thermal velocity for the (r, q) distributed plasma, and N is the total number density. The general dispersion relation of electrostatic waves is

$$1 - \sum_\alpha \frac{\omega_{p\alpha}^2}{k^2}\int_{-\infty}^{\infty}\frac{\partial f_\alpha/\partial v_z}{(v_z-\omega/k)}\,dv = 0, \quad (5)$$

where α is for either hot component 'h' or for cold component 'c'. Substituting Eq. (1) into Eq. (5), and integrating over v_x, v_y, and v_z, we obtain the general dispersion relation for the electrostatic waves modelled with generalized (r, q) distribution function as

$$1 + \frac{2\omega_p^2}{k^2}\left\{\frac{(1-F)}{\psi_{thc}^2}[H + \xi_c Z_1^{(r,q)}(\xi_c)] + \frac{F}{\psi_{thh}^2}[H + \xi_h Z_1^{(r,q)}(\xi_h)]\right\} = 0, \quad (6)$$

where

$$H = \frac{3(q-1)^{-1/(1+r)}\Gamma\left(q-\frac{1}{2(1+r)}\right)\Gamma\left(1+\frac{1}{2(1+r)}\right)}{2\Gamma\left(q-\frac{3}{2(1+r)}\right)\Gamma\left(1+\frac{3}{2(1+r)}\right)}, \quad (7)$$

and

$$Z_1^{(r,q)}(\xi_\alpha) = \frac{3(q-1)^{-3/2(1+r)}\Gamma(q)}{4\Gamma(q-3/2(1+r))\Gamma(1+3/2(1+r))} \times \int_{-\infty}^{\infty}\frac{ds}{(s_\alpha-\xi_\alpha)}\left(1+\frac{1}{q-1}s_{c,h}^{2(r+1)}\right)^{-q} \quad (8)$$

is the generalized plasma dispersion function for the (r, q) case.[49] Here $\xi_\alpha = \omega/k\psi_{th\alpha}$ and $s_\alpha = v/\psi_{th\alpha}$.

We have neglected the ion terms in Eq. (6) as it is justified to consider the ions as immobile giving a uniform background that simply maintains the charge neutrality for the Langmuir waves. Using the appropriate limiting form $\xi_\alpha \gg 1$ of the generalized plasma dispersion function (8), the dispersion relation for hot and cold species can be written as

$$D_r(\Omega) + iD_i(\Omega) = 0, \quad (9)$$

where the real and imaginary terms can be written as

$$D_r(\Omega) = 1 - \frac{1}{\Omega^2}[(1-F)+F] - \frac{2KDk^2\lambda_D^2}{\Omega^4} \times \left[(1-F)+\frac{T_h}{T_c}F\right], \quad (10)$$

and

$$D_i(\Omega) = \frac{2\pi\Omega C}{D^{3/2}k^3\lambda_D^3}\left[(1-F)\left(1+\frac{1}{q-1}\left\{\frac{\Omega^2}{Dk^2\lambda_D^2}\right\}^{r+1}\right)^{-q} + F\left(\frac{T_c}{T_h}\right)^{3/2}\left(1+\frac{1}{q-1}\left\{\frac{\Omega^2}{Dk^2\lambda_D^2}\frac{T_c}{T_h}\right\}^{r+1}\right)^{-q}\right], \quad (11)$$

respectively. Here $\Omega = \omega/\omega_p$, D is given by Eq. (3), and

$$K = \frac{3(q-1)^{1/(1+r)}\Gamma\left(q-\frac{5}{2(1+r)}\right)\Gamma\left(1+\frac{5}{2(1+r)}\right)}{10\Gamma\left(q-\frac{3}{2(1+r)}\right)\Gamma\left(1+\frac{3}{2(1+r)}\right)}. \quad (12)$$

The solution of $D_r(\Omega_r) = 0$ gives the real frequency Ω_r of the wave, which takes the following form only for the positive root:

$$\Omega_r \simeq \sqrt{\frac{1}{2} + \frac{1}{2}\left(1 + 8DKk^2\lambda_D^2\left(1 - F + \frac{T_h}{T_c}F\right)\right)^{1/2}}. \quad (13)$$

The damping rate of the wave is determined by the standard relationship

$$D_i \simeq -\frac{D_i}{\partial D_r/\partial\Omega}\bigg|_{\Omega_r}. \quad (14)$$

Substituting Eq. (13) into Eq. (14), the damping rate of the wave can be written as

$$\begin{aligned}\Omega_i = &-\frac{\pi C}{D^{3/2}}\frac{\Omega^8}{k^3\lambda_D^3}\left(\Omega^4 + 4KD\Omega^2k^2\lambda_D^2\left(1 - F + \frac{T_h}{T_c}F\right)\right)^{-1}\\ &\times\left[(1-F)\left(1 + \frac{1}{q-1}\left\{\frac{\Omega^2}{Dk^2\lambda_D^2}\right\}^{r+1}\right)^{-q}\right.\\ &\left.+F\left(\frac{T_c}{T_h}\right)^{3/2}\left(1 + \frac{1}{q-1}\left\{\frac{\Omega^2}{Dk^2\lambda_D^2}\frac{T_c}{T_h}\right\}^{r+1}\right)^{-q}\right]. \quad (15)\end{aligned}$$

In the long-wavelength limit,

$$\begin{aligned}&8KDk^2\lambda_D^2(1 - F + F(T_c/T_h)) \ll 1,\\ &\Omega_r \simeq \sqrt{1 + 2KDk^2\lambda_D^2(1 - F + F(T_c/T_h))},\end{aligned}$$

and equation (15) can be further reduced to

$$\begin{aligned}\Omega_i \simeq &-\frac{\pi C}{D^{3/2}}\frac{1}{k^3\lambda_D^3}\\ &\times\left[(1-F)\left(1 + \frac{1}{q-1}\left\{\frac{1}{Dk^2\lambda_D^2}\right.\right.\right.\\ &\left.\left.\left.+2K(1 - F + F(T_h/T_c))\right\}^{r+1}\right)^{-q}\right.\\ &+F\left(\frac{T_c}{T_h}\right)^{3/2}\left(1 + \frac{1}{q-1}\left\{\frac{1}{Dk^2\lambda_D^2}\left(\frac{T_c}{T_h}\right)\right.\right.\\ &\left.\left.\left.+2K(1 - F + F(T_h/T_c))\left(\frac{T_c}{T_h}\right)\right\}^{r+1}\right)^{-q}\right]. \quad (16)\end{aligned}$$

In the limit $r = 0$ and $q \to \infty$, the above equation is a solution of Maxwellian type.[50] Here we note that there is a slight change in the real frequency when we use generalized (r, q) distribution function, but the damping rate changes significantly and is strongly dependent on the spectral indices r and q.

4. Numerical solution

The numerical solution of Eq. (16) is shown in Figs. 3–6 for different values of r and q when 1% hot population at 10 eV is added to cold dense population at 1 eV for the limit $k\lambda_D \ll 1$ in the appropriate limiting form $\xi_\alpha \gg 1$ of the generalized plasma dispersion function (8). Figure 3 is plotted for different values of q when $r = 1$ corresponding to Fig. 1. From Fig. 3, we can see that the damping rate significantly increases when q decreases from 15 to 2. This is due to the fact that as the high-energy tail increases in the profile of distribution function, the damping rate increases for the low values of q (see Fig. 1). Compared with the Maxwellian damping rate, the (r, q) damping rate remains higher from Maxwellian in the range of $0.0 \le k\lambda_D < 0.25$ when $q < 5$, and then decreases for higher values of q. Thus, when $q < 5$, the small hot population in the non-Maxwellian distribution dominates, and damping rate increases relative to the Maxwellian rate. However, when $q \ge 5$, bulk population dominates over the small hot superthermal population in the non-Maxwellian distribution, and damping rate decreases relative to the Maxwellian.

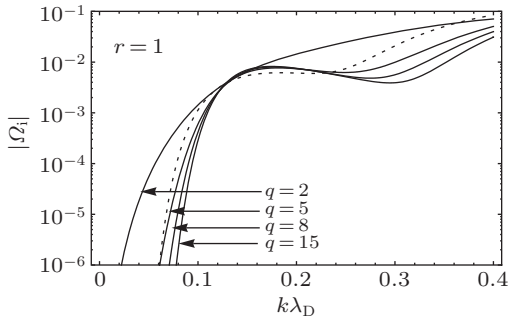

Fig. 3. Landau damping rates for different values of q when $r = 1$ corresponding to distribution functions shown in Fig. 1. Maxwellian damping rates are also given by dotted line for comparison.

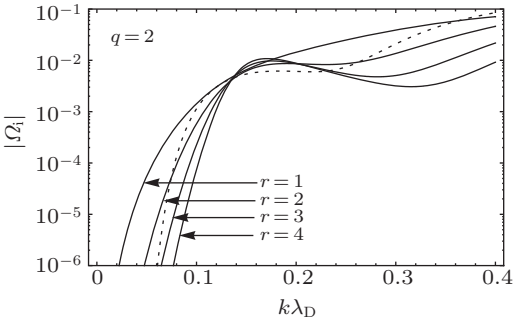

Fig. 4. Landau damping rates for different values of r when $q = 2$ corresponding to distribution functions shown in Fig. 2. Maxwellian damping rates are also given by dotted line for comparison.

Figure 4 depicts the magnitude of damping rates for different values of r when $q = 2$. We can see that the damping rate increases when r decreases from 4 to 1. This is due to the fact that as the flat part at low-energy region in the profile of distribution function decrease, effect of superthermal particles becomes more prominent (see Fig. 2). As compared to the Maxwellian damping rate, the (r, q) damping rate remains higher than the Maxwellian case in the range $0.0 \le k\lambda_D < 0.25$ when $r < 2$, and then decreases for higher values of r. Thus, when $r < 2$, the small hot superthermal population in the non-Maxwellian plasmas dominates, and the damping rate increases as compared to the Maxwellian rate,

but when $r > 2$, bulk population dominates the small hot superthermal population, and damping rate decreases as compared to the Maxwellian rate. Comparing Fig. 3 with Fig. 4 also shows that for fixed values of $k\lambda_D$, the damping rate significantly increases when the value of r or q decreases.

Figures 5 and 6 are plotted for negative values of r.[51,52] Figure 5(a) shows the profiles of generalized (r, q) distribution function for a 1% hot population at 10 eV added to cold dense population at 1 eV for different values of q when $r = -0.15$. We can see that as the value of q increases, the high-energy tail decreases, but remains higher in those profiles where we have used positive r values for the same values of spectral index q. Figure 5(b) shows the magnitude of damping rates corresponding to the distribution functions in the upper panel. We can note that the damping rate increases with the decrease in the value of q, but remains higher than the Maxwellian damping rate throughout the $k\lambda_D$ range. Figure 6 is plotted for different negative values of r for $q = 4$ when a 1% hot population at 10 eV added to cold dense population at 1 eV. Figure 6(a) shows the profiles of generalized (r, q) distribution function when $q = 4$. We can see that as the negative value of r increases, the high-energy tail increases, and the peak of the bulk distribution becomes sharper. The corresponding damping rates are shown in Fig. 6(b). The magnitude of damping rate decreases with the increase in the negative values of r except for a small range $k\lambda_D \leq 0.4$, where it increases with the increase in the negative values of r. However, compared with the Maxwellian damping rate, the (r, q) damping rate remains higher in the range $k\lambda_D < 0.3$ for all the negative values of r.

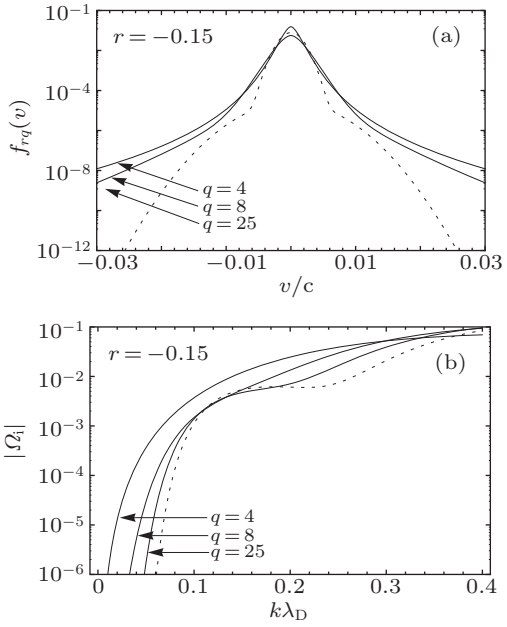

Fig. 5. (a) Profiles of generalized (r, q) distribution function for different values of q when $r = -0.15$ and (b) the corresponding damping rates for the same values of r and q when $F = 0.01$, $T_c = 1$ eV, and $T_h = 10$ eV. Maxwellian distribution and damping rate are given by the dotted line for comparison.

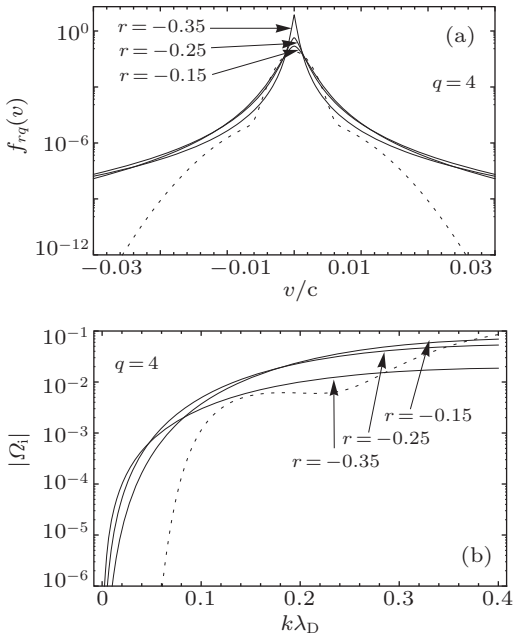

Fig. 6. (a) Profiles of generalized (r, q) distribution function for different values of r when $q = 4$ and (b) the corresponding damping rates for the same values of r and q when $F = 0.01$, $T_c = 1$ eV, and $T_h = 10$ eV. Maxwellian distribution and damping rate are given by the dotted line for comparison.

5. Limiting case

As mentioned above, in the limit $r = 0$ and $q = \kappa + 1$, Eq. (1) is reduced to kappa distribution function,[2,12] and in the limiting case $r = 0$ and $q \to \infty$, equation (1) is reduced to the well-known Maxwellian distribution function. We now plot the generalized (r, q) distribution function in these limits together to see how a distribution consisting of a purely Maxwellian core superimposed by a high-energy tail affects the pure Maxwellian damping rate. In Fig. 7, the cold bulk part of the distribution is plotted in the limit $r = 0$ and $q \to \infty$. That is to say, it represents the Maxwellian distribution function, and for the small bulk population, distribution is plotted in the limit $r = 0$ and $q = \kappa + 1$. In other words, it represents the kappa distribution function. Therefore, the complete distribution is a combination of a kappa distribution function superimposed on a cold bulk Maxwellian. We can see that as

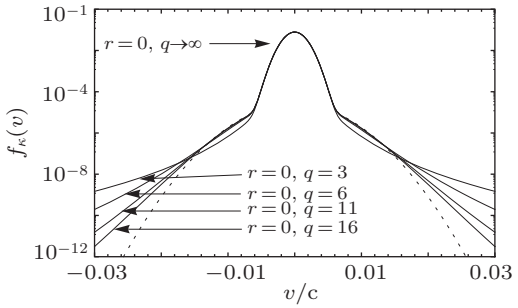

Fig. 7. Profiles of generalized (r, q) distribution function in the limiting cases when the cold bulk population represents Maxwellian distribution and a small hot population represents the kappa distribution function when $F = 0.01$, $T_c = 1$ eV, and $T_h = 10$ eV.

q or κ decreases, the high-energy tail of the distribution increases. Corresponding damping rates are plotted in Fig. 8, where we can see that damping rate significantly increases for all the values of q in the range $0.0 \leq k\lambda_D \leq 0.8$, and then becomes equal to the Maxwellian damping rate when $k\lambda_D > 0.8$.

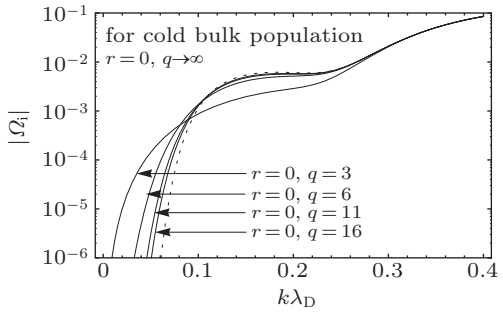

Fig. 8. Landau damping rates for the same parameters as that of Fig. 7. Enhancement of the Landau damping rates can be seen in the smaller wave numbers which becomes equal to Maxwellian damping rates as $k\lambda_D > 0.08$.

6. Comparison

Figure 9 shows the comparison between the magnitudes of damping rates when the distribution function contains a 1% hot population at 10 eV added to the 99% cold bulk population at 1 eV (solid line) and when the hot population is increased to 10% at 10 eV of the cold bulk population at 1 eV (bold solid line). We can see that as the percentage of hot population increases, a significant enhancement in the damping rate is clearly witnessed for all values of $k\lambda_D$. Therefore, for the larger fraction of the hot population (10%), the Landau damping is enhanced significantly for the generalized (r, q) distribution function.

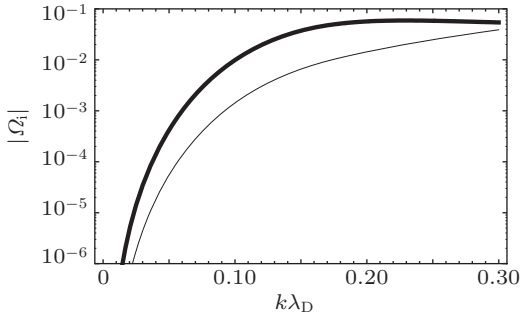

Fig. 9. Damping rates when the distribution function contains a 1% hot population at 10 eV added to the 99% cold bulk population at 1 eV (solid line) and when the hot population increases to 10% at 10 eV of the cold bulk population at 1 eV (bold solid line). Enhancement in the damping rate is clearly seen for higher temperatures of a small hot population.

Figure 10 depicts the comparison between the magnitudes of damping rates when the distribution function contains only one cold bulk population at 1 eV (dotted line), a 1% hot population at 10 eV added to the 99% cold bulk population at 1 eV (dashed line) and when a 10% hot population at 10 eV is added to the 90% of cold bulk population at 1 eV (solid line). We can see that the presence of a small hot population can significantly increase the damping rate as compared to the damping rate when the small hot population is absent from the distribution function. Further increase in the percentage of the hot population results in further enhancement of the damping rates.

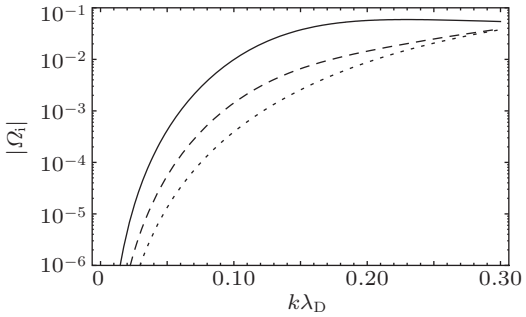

Fig. 10. Damping rates when the distribution function contains only one cold bulk population at 1 eV (dotted line), a 1% hot population at 10 eV added to the 99% cold bulk population at 1 eV (dashed line) and when a 10% hot population at 10 eV is added to the 90% of cold bulk population at 1 eV (solid line). A clear and considerable enhancement in the damping rates is witnessed due to the presence of a small hot population.

Figure 11 shows the comparison between the magnitudes of damping rates when the distribution function contains a 1% hot population at 10 eV (solid line), at 20 eV (dashed line), and at 30 eV (dotted line) added to the 99 % cold bulk population at 1 eV. We can see that as the temperature of the hot population increases, a significant enhancement in the damping rate is clearly witnessed for the values when $k\lambda_D < 0.15$. Comparison between Fig. 9 and Fig. 11 shows that damping is more pronounced for the density than the temperature of the hot population.

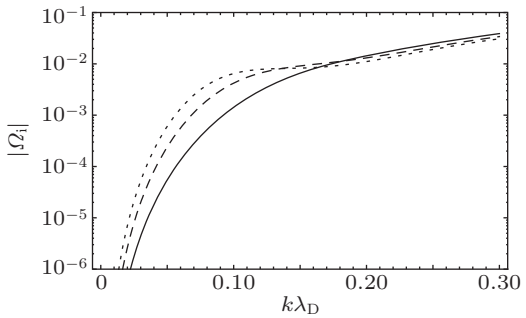

Fig. 11. Damping rates when the distribution function contains a 1% hot population at 10 eV (solid line), at 20 eV (dashed line) and at 30 eV (dotted line) added to the 99% cold bulk population at 1 eV. Enhancement in the damping rate is evident for the increase in temperature of the hot population when $k\lambda_D < 0.15$.

7. Discussion and conclusion

In plasmas where there exist two electron populations with different temperatures, both weak and strong damping

rates have been investigated modelled with generalized (r, q) distribution function under different density and temperature conditions and values of spectral indices as shown above. Comparison between Maxwellian distribution function and its corresponding damping rate is also given. The departure from the Maxwellian damping rate is strongly dependent on the spectral indices r and q for the generalized (r, q) distribution function. This has implications for plasmas like that of the solar wind, magnetosphere, and laboratory plasmas where such distributions are found.

Effects of two temperature plasmas are important for a wide range of temperature ratios and density variations. These, however, cannot be completely covered in a single study. Therefore, in this study, for numerical purposes we have considered 1% of a hot population at 10 eV and a cold dense population at 1 eV based on the following studies. For a one-dimensional particle-in-cell (PIC) simulation of beam–plasma interaction,[53] 0.1% of a hot population is produced at a temperature 10 times the cold bulk population temperature. Using these parameters, simulation results were in good agreement with their theoretical model. Moreover, Wickens *et al*.[54] have found that the hot to cold electron temperature ratios change from 6 to 10 while studying the ion emission from laser-produced plasmas with two electron temperatures. Kegel[55] also observed stronger Landau damping than in thermodynamic equilibrium when hot to cold electron temperature ratio is kept at 10 during the study of light scattering from plasmas with a non-Maxwellian velocity distribution. In a comprehensive study of solar wind electron distribution functions inside magnetic clouds,[33] the halo temperature has been found to be one order higher than the core electron temperature.

The enhancement in Landau damping rates of Langmuir waves for the generalized (r, q) distribution function in the small wave number $k\lambda_{\rm D} < 0.1$ is explained. Here the phase velocity of the wave is superthermal, and high-energy particles in the tail of the distribution readily absorb energy from the wave. In this velocity region, the generalized (r, q) distribution function contain power law tail whose slope (in magnitude) decreases with increasing q or r, which explains why smaller values of q and r enhances damping in the small wave number region. Varying r or q not only changes the slope of the distribution function but also the phase velocity of the wave. The former occurs nonuniformly in the velocity space, while the latter in k space. The interplay between these two nonuniform variations gives rise to the complicated dependence of damping rates on r or q in intermediate wave numbers $0.1 < k\lambda_{\rm D} < 0.2$. Therefore, the high phase velocity of the Langmuir wave in the small wave number region ensures that such waves couple strongly to a small hot electron population in the tail of the distribution with a resulting enhancement in the damping as compared to the Maxwellian damping rate. Thus, a highly non-Maxwellian electron VDFs favour the observations of shorter wavelength Langmuir waves in laboratory and space plasmas as compared to the Maxwellian plasmas. Whereas, Maxwellian plasmas favour the observations of long wavelength Langmuir waves as compared to the non-Maxwellian plasmas. However, the electromagnetic picture can alter the picture determined by a purely electrostatic picture. Thus, the theoretical model presented here may be helpful in understanding Langmuir waves damping with non-Maxwellian distributions in a variety of plasmas, where such waves are observed experimentally,[56] in the auroral zone,[44] Earth's bow shock,[45] interplanetary shocks,[46] and in the solar wind.[47,48]

References

[1] Landau L D 1946 *J. Phys*. **10** 25
[2] Thorne R M and Summers D 1991 *Phys. Fluids B* **3** 2117
[3] Qureshi M N S, Shi J K and Ma S Z 2005 *Phys. Plasmas* **12** 122902
[4] Gosling J T, Ashbridge J R, Bame S J, Feldman W C and Zwickl R D 1981 *J. Geophys. Res.* **86** 547
[5] Lin R P, Levedahi W K, Lotko W, Gurnett D A and Scarf F L 1986 *Astrophys. J.* **308** 954
[6] Vasyliunas V M 1990 *J. Geophys. Res.* **73** 2839
[7] Fitzenreiter R J, Ogilivie K W, Chornay D J and Keller J 1998 *Geophys. Res. Lett.* **25** 249
[8] Feldman W C, Bame S J, Gary S P, Gosling J T, McComas D, Thomsen M F, Paschmann G, Sckopke N, Hoppe M M and Russell C T 1982 *Phys. Res. Lett.* **49** 199
[9] Feldman W C, Anderson R C, Bame S J, Gosling J T and Zwickl R D 1983 *J. Geophys. Res.* **88** 9949
[10] Montgomery M D, Asbridge J R and Bame S J 1970 *Geophys. Res. Lett.* **75** 1217
[11] Montgomery M D 1970 *Particles and Fields in the Magnetosphere* (Hingham: Mass) p. 95
[12] Summers D and Thorne R M 1991 *Phys. Fluids* B **3** 1835
[13] Mace R L and Hellberg M A1995 *Phys. Plasmas* **2** 2098
[14] Maksimovic M, Pierrard V and Riley P 1997 *Geophys. Res. Lett.* **24** 1151
[15] Qureshi M N S, Pallocchia G, Bruno R, Cattaneo M B, Formisano V, Shah H A, Reme H, Bosued J M, Dandouras I, Sauvaud J A, Kistler L, Moebius E, Klecker B, Carlson CW, McFadden J P, Parks G K, McCarthy M, Korth A, Lundin R and Balogh A 2003 *AIP Conference Proceedings Solar Wind* p. 679
[16] Hasegawa A, Mima K and Duong-van M 1998 *Phys. Rev. Lett.* **25** 4099
[17] Treumann R A 1999 *Phys. Scr.* **59** 19
[18] Treumann R A 1999 *Phys. Scr.* **59** 204
[19] Collier M R 1993 *Geophys. Res. Lett.* **20** 1531
[20] Freund H P, Smith R A and Papadopoulos K 1981 *Phys. Fluids* **24** 442
[21] Fourkal E, Bychenkov V Y, Rozmus W, Sydora R, Kirkby C, Capjack C E, Glenzer S H and Baldis H A 2001 *Phys. Plasmas* **8** 550
[22] Tanaka M and Papadopoulos K1983 *Phys. Fluids* **26** 1697
[23] Wang J G, Newman D L and Goldman M V 1997 *J. Atmos. Sol. Terr. Phys.* **59** 2461
[24] Afeyan B B, Chou A E, Matte J P, Town R P J and Kruer W J 1998 *Phys. Rev. Lett.* **80** 2322
[25] Yoon P H, Rhee T and Ryu C M 2005 *Phys. Rev. Lett.* **95** 215003
[26] Lin R P 1980 *Sol. Phys.* **67** 393
[27] Lin R P 1998 *Space Sci. Rev.* **86** 61
[28] Pierrard V, Maksimovic M and Lemaire J 2001 *Astrophys. Space Sci.* **277** 195
[29] Pagel C, Crooker N U, Larson D E, Kahler S W and Qwens M J 2005 *J. Geophys. Res.* **110** A01103
[30] Gaelzer R, Ziebell L F, Vinas A F, Yoon P H and Ryu C M 2008 *Astrophys. J.* **677** 676
[31] Philipp W G, Miggenrieder H and Montgomery M D 1987 *J. Geophys. Res.* **92** 1075
[32] Pierrard V, Maksimovic M and Lemaire J 2001 *Astrophys. Space Sci.* **277** 195

[33] Nieves-Chinchilla T and Vinas A F 2008 *J. Geophys. Res.* **113** A02105
[34] Parks G K, Lee E, Lin N, Mozer F, Wilber M, Dandouras I, Reme H, Lucek E, Fazakerley A, Goldstein M, Gurgiolo C, Canu P, Cornilleau-Wehrlin N and Decreau P 2007 *Phys. Rev. Lett.* **98** 265001
[35] Khan S A and Haque A 2008 *Chin. Phys. Lett*. **12** 4329
[36] Hussain S, Akhtar A and Saeed-ur-Rehman 2011 *Chin. Phys. Lett*. **4** 045202
[37] Mirza Arshad M, Mahmood S and Khan S A 2009 *Chin. Phys. Lett*. **4** 045203
[38] Duan P, Yu D R, Qing S W, Ding Y J and Wang X G 2011 *Acta Phys. Sin.* **60** 025204 (in Chinese)
[39] Duan P, Zhao X Y, Ni Z X and Liu J Y *Acta Phys. Sin.* 2011 **60** 045205 (in Chinese)
[40] Mace R L and Hellberg M A 2003 *Phys. Plasmas* **10** 21
[41] Bers A, Shkarofsky I P and Shoucri M 2009 *Phys. Plasmas* **16** 022104
[42] Xiao Z, Wang W Q and Hao Y Q 2004 *Chin. Phys. Lett.* **21** 2461
[43] Ouazene M and Annou R 2011 *Phys. Plasmas* **18** 114502
[44] Bonnell J, Kintner P, Wahlund J E and Holtet J A 1997 *J. Geophys. Res.* **102** 17233
[45] Bale S D, Burgess D, Kellogg P J, Goetz K and Monson S J 1997 *J. Geophys. Res.* **102** 11281
[46] Pulupa M P, Bale S D and Kasper J C 2010 *J. Geophys. Res*. **115** A04106
[47] Thejappa G and MacDowall R J 2000 *Astrophys. J.* **544** L163
[48] MacDowall R J, Lin N G and McComas D J 2003 *Adv. Space Res.* **32** 479
[49] Qureshi M N S, Shah H A, Murtaza G, Scwartz S J and Mahmood F 2004 *Phys. Plasmas* **11** 3819
[50] Rose D V, Guillory J and Beall J H 2005 *Phys. Plasmas* **12** 014501
[51] Kiran Z, Shah H A, Qureshi M N S and Murtaza G 2006 *Solar Phys.* **236** 167
[52] Mushtaq A and Shah H A 2006 *Phys. Plasmas* **13** 012303
[53] Rose D V, Guillory J U and Beall J H 2002 *Phys. Plasmas* **9** 1000
[54] Wickens L M, Allen J E and Rumsby P T 1978 *Phys. Rev. Lett.* **41** 243
[55] Kegel W H 1970 *Plasma Phys.* **12** 295
[56] Liu Z J, Xiang J, Zheng C Y, Zhu S P, Cao L H, He X T and Wang Y G 2010 *Chin. Phys. B* **19** 075201